Can the newly reported $P_{cs}(4459)$ be a strange hidden-charm $\Xi_c\bar{D}^*$ molecular pentaquark?

Rui Chen[1,2,*]

[1]*Center of High Energy Physics, Peking University, Beijing 100871, China*
[2]*School of Physics and State Key Laboratory of Nuclear Physics and Technology, Peking University, Beijing 100871, China*

(Received 18 November 2020; accepted 12 February 2021; published 4 March 2021)

Stimulated by the $P_{cs}(4459)$ reported by the LHCb collaboration, we perform a single $\Xi_c\bar{D}^*$ channel and a coupled $\Xi_c\bar{D}^*/\Xi_c^*\bar{D}/\Xi_c'\bar{D}^*/\Xi_c^*\bar{D}^*$ channel analysis by using a one-boson-exchange model. Our results indicate that the newly $P_{cs}(4459)$ cannot be a pure $\Xi_c\bar{D}^*$ molecular state, but a coupled $\Xi_c\bar{D}^*/\Xi_c^*\bar{D}/\Xi_c'\bar{D}^*/\Xi_c^*\bar{D}^*$ bound state with $I(J^P) = 0(3/2^-)$, where the $\Xi_c\bar{D}^*$ and $\Xi_c^*\bar{D}$ components are dominant. Meanwhile, we find the interactions from the $\Xi_c'\bar{D}^*$ system with $0(1/2^-)$, the $\Xi_c^*\bar{D}$ system with $1(3/2^-)$, and the $\Xi_c^*\bar{D}^*$ system with $1(1/2^-)$ are strongly attractive, where one can expect possible strange hidden-charm molecular or resonant structures near these thresholds with the assigned quantum numbers.

DOI: 10.1103/PhysRevD.103.054007

I. INTRODUCTION

In 2019, the LHCb collaboration updated the observations in the $\Lambda_b^0 \to J/\psi p K^-$ process by using more data [1], they not only discovered a new narrow pentaquark state, $P_c(4312)^+$, but also found that the $P_c(4450)$ reported previously [2] consists of two narrow overlapping peaks, $P_c(4440)^+$ and $P_c(4457)^+$.

The discovery of P_c states has sparked an enormous interest in the study of multiquark systems and exotic hadrons. Several possible explanations have been put forward in the literature: the molecular states [3–11], the compact pentaquark states [12–18], and the kinematical effects [19,20] (see review papers [21–26] for more details). In fact, before the observations of the P_c states, the hidden-charm pentaquarks were predicted in Refs. [27–31].

Among the different interpretations to these P_c states, the hadronic molecular state assignments to them are the most popular one. The masses of the P_c states are close to the thresholds of a charmed baryon and an anticharmed meson, which is the main reason why the hadronic molecular state assignments to them were proposed. For example, $P_c(4312)$, $P_c(4440)$, and $P_c(4457)$ are regarded as the hidden-charm molecular pentaquarks, they are mainly composed by the $\Sigma_c\bar{D}$ state with $I(J^P) = 1/2(1/2^-)$, the $\Sigma_c\bar{D}^*$ state with $1/2(1/2^-)$ and $1/2(3/2^-)$, respectively [6].

Very recently, the LHCb collaboration reported evidence of the $P_{cs}(4459)$ in $\Xi_b^- \to J/\psi\Lambda K^-$ with a 3.1σ statistical significant [32]. Its mass and width are

$$M = 4458.8 \pm 2.9^{+4.7}_{-1.2}\ \text{MeV}, \qquad \Gamma = 17.3 \pm 6.5^{+8.0}_{-5.7}\ \text{MeV},$$

respectively. Its spin parity was not determined yet. According to the decay final states $J/\psi\Lambda$, the $P_{cs}(4459)$ is a strange hidden-charm pentaquark containing $c\bar{c}sud$ valence quark components. Since its mass is just below the $\Xi_c\bar{D}^*$ threshold with around 19 MeV, whether the newly $P_{cs}(4459)$ can be explained as a strange hidden-charm $\Xi_c\bar{D}^*$ molecule is open to discussion [33–35], i.e., Chen *et al.*'s results supported the $P_{cs}(4459)$ as the $\Xi_c\bar{D}^*$ molecule of either $J^P = 1/2^-$ or $3/2^-$ after adopting the QCD sum rules [33].

In fact, many groups have predicted the existence of the strange hidden-charm pentaquarks [36–46], and proposed to search for the P_{cs} states in the $\Lambda_b(\Xi_b) \to J/\psi\Lambda K(\eta)$ [40,41,47]. Especially, Wang *et al.* predicted two isoscalar $\Xi_c\bar{D}^*$ molecular states with the chiral effective field theory [37], the masses of $\Xi_c\bar{D}^*$ molecules with $J^P = 1/2^-$ and $3/2^-$ are $4456.9^{+3.2}_{-3.3}$ and $4463.0^{+2.8}_{-3.0}$ MeV, respectively.

As we mentioned, the long range interaction from one pseudoscalar meson exchange is suppressed in the single $\Xi_c\bar{D}^*$ system [42]. In this work, we will give a more comprehensive and systematic investigation of the molecular explanation of the $P_{cs}(4459)$ after absorbing more effects. We still adopt the one-boson-exchange (OBE) model (including the π, σ, η, ρ, and ω exchanges), and adopt the $S-D$ wave mixing and the coupled-channel effect. By studying the hadronic molecular state assignment

*chen_rui@pku.edu.cn

to the $P_{cs}(4459)$, we want to further identify this molecular pentaquark configuration, especially the corresponding spin-parity quantum numbers.

This paper is organized as follows. After this introduction, we illustrate the deducing of the OBE effective potentials in Sec. II. The corresponding numerical results for the single $\Xi_c\bar{D}^*$ channel case and the coupled $\Xi_c\bar{D}^*/\Xi_c^*\bar{D}/\Xi_c'\bar{D}^*/\Xi_c^*\bar{D}^*$ case are given in Secs. III and IV, respectively. The paper ends with a summary in Sec. IV.

II. ONE-BOSON-EXCHANGE EFFECTIVE POTENTIALS

According to the heavy quark symmetry and chiral symmetry [48–53], the relevant effective Lagrangians are constructed as

$$\begin{aligned}\mathcal{L}_H &= g_S\langle\bar{H}_a^{(\bar{Q})}\sigma H_b^{(\bar{Q})}\rangle + ig\langle\bar{H}_a^{(\bar{Q})}\gamma_\mu A_{ab}^\mu\gamma_5 H_b^{(\bar{Q})}\rangle \\ &\quad - i\beta\langle\bar{H}_a^{(\bar{Q})}v_\mu(\mathcal{V}_{ab}^\mu-\rho_{ab}^\mu)H_b^{(\bar{Q})}\rangle \\ &\quad + i\lambda\langle\bar{H}_a^{(\bar{Q})}\sigma_{\mu\nu}F^{\mu\nu}(\rho)H_b^{(\bar{Q})}\rangle, \end{aligned} \tag{1}$$

$$\mathcal{L}_{\mathcal{B}_{\bar{3}}} = l_B\langle\bar{\mathcal{B}}_{\bar{3}}\sigma\mathcal{B}_{\bar{3}}\rangle + i\beta_B\langle\bar{\mathcal{B}}_{\bar{3}}v^\mu(\mathcal{V}_\mu-\rho_\mu)\mathcal{B}_{\bar{3}}\rangle, \tag{2}$$

$$\begin{aligned}\mathcal{L}_{\mathcal{B}_6} &= l_S\langle\bar{\mathcal{S}}_\mu\sigma\mathcal{S}^\mu\rangle - \frac{3}{2}g_1\varepsilon^{\mu\nu\lambda\kappa}v_\kappa\langle\bar{\mathcal{S}}_\mu A_\nu\mathcal{S}_\lambda\rangle \\ &\quad + i\beta_S\langle\bar{\mathcal{S}}_\mu v_\alpha(\mathcal{V}_{ab}^\alpha-\rho_{ab}^\alpha)\mathcal{S}^\mu\rangle + \lambda_S\langle\bar{\mathcal{S}}_\mu F^{\mu\nu}(\rho)\mathcal{S}_\nu\rangle, \end{aligned} \tag{3}$$

$$\mathcal{L}_{\mathcal{B}_{\bar{3}}\mathcal{B}_6} = ig_4\langle\bar{\mathcal{S}}^\mu A_\mu\mathcal{B}_{\bar{3}}\rangle + i\lambda_I\varepsilon^{\mu\nu\lambda\kappa}v_\mu\langle\bar{\mathcal{S}}_\nu F_{\lambda\kappa}\mathcal{B}_{\bar{3}}\rangle + \text{H.c.} \tag{4}$$

Here, the multiplet field $H^{(\bar{Q})}$ is composed by the pseudoscalar meson $\tilde{\mathcal{P}} = (\bar{D}^0, D^-)^T$ and the vector meson $\tilde{\mathcal{P}}^* = (\bar{D}^{*0}, D^{*-})^T$, while its conjugate field of $\bar{H}^{(\bar{Q})}$ satisfies $\bar{H}^{(\bar{Q})} = \gamma_0 H^{(\bar{Q})\dagger}\gamma_0$, and $\mathcal{S}$ is defined as a superfield, which includes $\mathcal{B}_6$ with $J^P = 1/2^+$ and $\mathcal{B}_6^*$ with $J^P = 3/2^+$ in the 6_F flavor representation. Their expressions read as

$$H^{(\bar{Q})} = [\tilde{\mathcal{P}}^{*\mu}\gamma_\mu - \tilde{\mathcal{P}}\gamma_5]\frac{1-\not{v}}{2}, \tag{5}$$

$$\mathcal{S}_\mu = -\sqrt{\frac{1}{3}}(\gamma_\mu + v_\mu)\gamma^5\mathcal{B}_6 + \mathcal{B}_{6\mu}^*. \tag{6}$$

The expressions of the axial current and the vector current are

$$\begin{aligned}A_\mu &= \frac{1}{2}(\xi^\dagger\partial_\mu\xi - \xi\partial_\mu\xi^\dagger) = \frac{i}{f_\pi}\partial_\mu\mathbb{P} + \cdots, \\ V_\mu &= \frac{1}{2}(\xi^\dagger\partial_\mu\xi - \xi\partial_\mu\xi^\dagger) = \frac{i}{2f_\pi^2}[\mathbb{P}, \partial_\mu\mathbb{P}] + \cdots, \end{aligned}$$

respectively, with $\xi = \exp(i\mathbb{P}/f_\pi)$ and the pion decay constant $f_\pi = 132$ MeV. $\rho_{ba}^\mu = ig_V\mathbb{V}_{ba}^\mu/\sqrt{2}$, $F^{\mu\nu}(\rho) = \partial^\mu\rho^\nu - \partial^\nu\rho^\mu + [\rho^\mu, \rho^\nu]$. $\mathbb{P}$ and $\mathbb{V}$ stand for the isoscalar and vector matrices, respectively. In the above formulas, the matrices $\mathcal{B}_{\bar{3}}$, $\mathcal{B}_6^{(\prime,*)}$, $\mathbb{P}$, and $\mathcal{V}$ are written as

$$\mathcal{B}_{\bar{3}} = \begin{pmatrix} 0 & \Lambda_c^+ & \Xi_c^+ \\ -\Lambda_c^+ & 0 & \Xi_c^0 \\ -\Xi_c^+ & -\Xi_c^0 & 0 \end{pmatrix},$$

$$\mathcal{B}_6^{(\prime,*)} = \begin{pmatrix} \Sigma_c^{(*)++} & \frac{1}{\sqrt{2}}\Sigma_c^{(*)+} & \frac{1}{\sqrt{2}}\Xi_c^{(\prime,*)+} \\ \frac{1}{\sqrt{2}}\Sigma_c^{(*)+} & \Sigma_c^{(*)0} & \frac{1}{\sqrt{2}}\Xi_c^{(\prime,*)0} \\ \frac{1}{\sqrt{2}}\Xi_c^{(\prime,*)+} & \frac{1}{\sqrt{2}}\Xi_c^{(\prime,*)0} & \Omega_c^{(*)0} \end{pmatrix},$$

$$\mathbb{P} = \begin{pmatrix} \frac{\pi^0}{\sqrt{2}} + \frac{\eta}{\sqrt{6}} & \pi^+ & K^+ \\ \pi^- & -\frac{\pi^0}{\sqrt{2}} + \frac{\eta}{\sqrt{6}} & K^0 \\ K^- & \bar{K}^0 & -\frac{2}{\sqrt{6}}\eta \end{pmatrix},$$

$$V = \begin{pmatrix} \frac{\rho^0}{\sqrt{2}} + \frac{\omega}{\sqrt{2}} & \rho^+ & K^{*+} \\ \rho^- & -\frac{\rho^0}{\sqrt{2}} + \frac{\omega}{\sqrt{2}} & K^{*0} \\ K^{*-} & \bar{K}^{*0} & \phi \end{pmatrix}.$$

By expanding Eqs. (1)–(4), one can further get

$$\mathcal{L}_{\tilde{\mathcal{P}}^{(*)}\tilde{\mathcal{P}}^{(*)}\sigma} = -2g_S\tilde{\mathcal{P}}_b^\dagger\tilde{\mathcal{P}}_b\sigma - 2g_S\tilde{\mathcal{P}}_b^*\cdot\tilde{\mathcal{P}}_b^{*\dagger}\sigma, \tag{7}$$

$$\begin{aligned}\mathcal{L}_{\tilde{\mathcal{P}}^{(*)}\tilde{\mathcal{P}}^{(*)}\mathbb{P}} &= \frac{2g}{f_\pi}(\tilde{\mathcal{P}}_{a\lambda}^{*\dagger}\tilde{\mathcal{P}} + \tilde{\mathcal{P}}_a^\dagger\tilde{\mathcal{P}}_{b\lambda}^*)\partial^\lambda\mathbb{P}_{ab} \\ &\quad + i\frac{2g}{f_\pi}v^\alpha\varepsilon_{\alpha\mu\nu\lambda}\tilde{\mathcal{P}}_a^{*\mu\dagger}\tilde{\mathcal{P}}_b^{*\lambda}\partial^\nu\mathbb{P}_{ab}, \end{aligned} \tag{8}$$

$$\begin{aligned}\mathcal{L}_{\tilde{\mathcal{P}}^{(*)}\tilde{\mathcal{P}}^{(*)}\mathbb{V}} &= \sqrt{2}\beta g_V\tilde{\mathcal{P}}_a^\dagger\tilde{\mathcal{P}}_b v\cdot\mathbb{V}_{ab} \\ &\quad - 2\sqrt{2}\lambda g_V v^\lambda\varepsilon_{\lambda\mu\alpha\beta}(\tilde{\mathcal{P}}_a^{*\mu\dagger}\tilde{\mathcal{P}}_b + \tilde{\mathcal{P}}_a^\dagger\tilde{\mathcal{P}}_b^{*\mu})\partial^\alpha\mathbb{V}_{ab}^\beta \\ &\quad - \sqrt{2}\beta g_V\tilde{\mathcal{P}}_a^{*\dagger}\cdot\tilde{\mathcal{P}}_b^* v\cdot\mathbb{V}_{ab} \\ &\quad - i2\sqrt{2}\lambda g_V\tilde{\mathcal{P}}_a^{*\mu\dagger}\tilde{\mathcal{P}}_b^{*\nu}(\partial_\mu\mathbb{V}_\nu - \partial_\nu\mathbb{V}_\mu), \end{aligned} \tag{9}$$

$$\mathcal{L}_{\mathcal{B}_{\bar{3}}\mathcal{B}_{\bar{3}}\sigma} = l_B\langle\bar{\mathcal{B}}_{\bar{3}}\sigma\mathcal{B}_{\bar{3}}\rangle, \tag{10}$$

$$\begin{aligned}\mathcal{L}_{\mathcal{B}_6^{(*)}\mathcal{B}_6^{(*)}\sigma} &= -l_S\langle\bar{\mathcal{B}}_6^{(\prime)}\sigma\mathcal{B}_6^{(\prime)}\rangle + l_S\langle\bar{\mathcal{B}}_{6\mu}^*\sigma\mathcal{B}_6^{*\mu}\rangle \\ &\quad - \frac{l_S}{\sqrt{3}}\langle\bar{\mathcal{B}}_{6\mu}^*\sigma(\gamma^\mu + v^\mu)\gamma^5\mathcal{B}_6^{(\prime)}\rangle + \text{H.c.}, \end{aligned} \tag{11}$$

$$\mathcal{L}_{\mathcal{B}_{\bar{3}}\mathcal{B}_{\bar{3}}V} = \frac{1}{\sqrt{2}}\beta_B g_V\langle\bar{\mathcal{B}}_{\bar{3}}v\cdot V\mathcal{B}_{\bar{3}}\rangle, \tag{12}$$

$$\begin{aligned}\mathcal{L}_{\mathcal{B}_6^{(*)}\mathcal{B}_6^{(*)}P} &= i\frac{g_1}{2f_\pi}\varepsilon^{\mu\nu\lambda\kappa}v_\kappa\langle\bar{\mathcal{B}}_6^{(\prime)}\gamma_\mu\gamma_\lambda\partial_\nu P\mathcal{B}_6^{(\prime)}\rangle \\ &\quad + i\frac{\sqrt{3}}{2}\frac{g_1}{f_\pi}v_\kappa\varepsilon^{\mu\nu\lambda\kappa}\langle\bar{\mathcal{B}}_{6\mu}^*\partial_\nu P\gamma_\lambda\gamma^5\mathcal{B}_6^{(\prime)}\rangle + \text{H.c.} \\ &\quad - i\frac{3g_1}{2f_\pi}\varepsilon^{\mu\nu\lambda\kappa}v_\kappa\langle\bar{\mathcal{B}}_{6\mu}^*\partial_\nu P\mathcal{B}_{6\lambda}^*\rangle, \end{aligned} \tag{13}$$

$$\begin{aligned}\mathcal{L}_{\mathcal{B}_6^{(*)}\mathcal{B}_6^{(*)}V} &= -\frac{\beta_S g_V}{\sqrt{2}}\langle\bar{\mathcal{B}}_6^{(\prime)} v\cdot V\mathcal{B}_6^{(\prime)}\rangle - i\frac{\lambda g_V}{3\sqrt{2}}\langle\bar{\mathcal{B}}_6^{(\prime)}\gamma_\mu\gamma_\nu(\partial^\mu V^\nu-\partial^\nu V^\mu)\mathcal{B}_6^{(\prime)}\rangle \\ &-\frac{\beta_S g_V}{\sqrt{6}}\langle\bar{\mathcal{B}}^*_{6\mu} v\cdot V(\gamma^\mu+v^\mu)\gamma^5\mathcal{B}_6^{(\prime)}\rangle - i\frac{\lambda_S g_V}{\sqrt{6}}\langle\bar{\mathcal{B}}^*_{6\mu}(\partial^\mu V^\nu-\partial^\nu V^\mu)(\gamma_\nu+v_\nu)\gamma^5\mathcal{B}_6^{(\prime)}\rangle \\ &+\frac{\beta_S g_V}{\sqrt{2}}\langle\bar{\mathcal{B}}^*_{6\mu} v\cdot V\mathcal{B}_6^{*\mu}\rangle + i\frac{\lambda_S g_V}{\sqrt{2}}\langle\bar{\mathcal{B}}^*_{6\mu}(\partial^\mu V^\nu-\partial^\nu V^\mu)\mathcal{B}^*_{6\nu}\rangle + \text{H.c.},\end{aligned} \tag{14}$$

$$\begin{aligned}\mathcal{L}_{\mathcal{B}_{\bar{3}}\mathcal{B}_6^{(*)}V} &= -\frac{\lambda_I g_V}{\sqrt{6}}\varepsilon^{\mu\nu\lambda\kappa}v_\mu\langle\bar{\mathcal{B}}_6^{(\prime)}\gamma^5\gamma_\nu(\partial_\lambda V_\kappa-\partial_\kappa V_\lambda)\mathcal{B}_{\bar{3}}\rangle \\ &-\frac{\lambda_I g_V}{\sqrt{2}}\varepsilon^{\mu\nu\lambda\kappa}v_\mu\langle\bar{\mathcal{B}}^*_{6\nu}(\partial_\lambda V_\kappa-\partial_\kappa V_\lambda)\mathcal{B}_{\bar{3}}\rangle + \text{H.c.},\end{aligned} \tag{15}$$

$$\begin{aligned}\mathcal{L}_{\mathcal{B}_{\bar{3}}\mathcal{B}_6^{(*)}P} &= -\sqrt{\frac{1}{3}}\frac{g_4}{f_\pi}\langle\bar{\mathcal{B}}_6^{(\prime)}\gamma^5(\gamma^\mu+v^\mu)\partial_\mu P\mathcal{B}_{\bar{3}}\rangle \\ &-\frac{g_4}{f_\pi}\langle\bar{\mathcal{B}}^*_{6\mu}\partial^\mu P\mathcal{B}_{\bar{3}}\rangle + \text{H.c.},\end{aligned} \tag{16}$$

which will be applied to the deduction of scattering amplitudes.

$g_s=\tilde{g}/2\sqrt{6}$, $\tilde{g}$ is the coupling for the process $D(0^+)\to D(0^-)+\pi$ [54]. β is fixed as $\beta=0.9$ according to vector meson dominance [55], and λ is determined through a comparison of the form factor between the theoretical calculation from the light cone sum rule and lattice QCD [55]. For the π exchange couplings, they are extracted from the decay width of $D^*\to D\pi$, $\Sigma_c\to\Lambda_c\pi$, and $\Sigma_c^*\to\Lambda_c\pi$ [53,55,56]. The remaining coupling constants relevant to the heavy baryons can be estimated by borrowing the nucleon-nucleon interaction in the quark level [53]. Their values are collected in Table I.

In a Breit approximation, the effective potentials in the momentum space can be related to the corresponding scattering amplitudes, i.e.,

$$\mathcal{V}_E^{h_1h_2\to h_3h_4}(\boldsymbol{q}) = -\frac{\mathcal{M}(h_1h_2\to h_3h_4)}{\sqrt{\prod_i 2M_i\prod_f 2M_f}}, \tag{17}$$

where M_i and M_f stand for the masses of the initial states (h_1, h_2) and final states (h_3, h_4), respectively. After performing a Fourier transformation, we obtain the effective potential in the coordinate space $\mathcal{V}(\boldsymbol{r})$,

TABLE I. Coupling constants adopted in our calculation.

l_B	$\beta_B g_V$	l_S	g_1	$\lambda_S g_V(\text{GeV}^{-1})$	βg_V
−3.65	−6.00	7.30	1.00	19.20	5.22
$\beta_S g_V$	g_S	g_4	$\lambda_I g_V(\text{GeV}^{-1})$	$\lambda g_V(\text{GeV}^{-1})$	
12.00	0.76	1.06	−6.80	3.25	

$$\mathcal{V}_E^{h_1h_2\to h_3h_4}(\boldsymbol{r}) = \int\frac{d^3\boldsymbol{q}}{(2\pi)^3}e^{i\boldsymbol{q}\cdot\boldsymbol{r}}\mathcal{V}_E^{h_1h_2\to h_3h_4}(\boldsymbol{q})\mathcal{F}^2(q^2,m_E^2).$$

Here, we introduce a monopole form factor $\mathcal{F}(q^2,m_E^2)=(\Lambda^2-m_E^2)/(\Lambda^2-q^2)$ at every interactive vertex, it expresses the off-shell effect of the exchanged boson. Λ, m_E, and q are the cutoff, mass, and four-momentum of the exchanged meson, respectively. As we discussed in Ref. [57], there are other kinds of form factors adopted to study the hadron-hadron interactions, like the dipole and the exponential forms. For the cutoff, it is a phenomenological parameter. According to the experience of the deuteron, Λ in the monopole form factor is taken around 1 GeV [58,59].

For the S-wave $\Xi_c\bar{D}^*$ system, its spin parity can be either $J^P=1/2^-$ or $3/2^-$. When we consider the $S-D$ wave mixing effect, the spin-orbit wave functions are

$$\begin{aligned}J^P &= \frac{1^-}{2}:|^2\mathbb{S}_{\frac{1}{2}}\rangle,\quad |^4\mathbb{D}_{\frac{1}{2}}\rangle|^6\mathbb{D}_{\frac{1}{2}}\rangle, \\ J^P &= \frac{3^-}{2}:|^4\mathbb{S}_{\frac{3}{2}}\rangle,\quad |^2\mathbb{D}_{\frac{3}{2}}\rangle,\quad |^4\mathbb{D}_{\frac{3}{2}}\rangle|^6\mathbb{D}_{\frac{3}{2}}\rangle.\end{aligned} \tag{18}$$

The flavor wave functions $|I,I_3\rangle$ of these discussed systems are

$$\Xi_c^{(\prime,*)}\bar{D}^*:\begin{cases}|1,1\rangle = |\Xi_c^{(\prime,*)+}\bar{D}^{*0}\rangle, \\ |1,0\rangle = \frac{1}{\sqrt{2}}(|\Xi_c^{(\prime,*)+}D^{*-}\rangle + |\Xi_c^{(\prime,*)0}\bar{D}^{*0}\rangle), \\ |1,-1\rangle = |\Xi_c^{(\prime,*)0}D^{*-}\rangle, \\ |0,0\rangle = \frac{1}{\sqrt{2}}(|\Xi_c^{(\prime,*)+}D^{*-}\rangle - |\Xi_c^{(\prime,*)0}\bar{D}^{*0}\rangle),\end{cases} \tag{19}$$

where I and I_3 are the isospin and its third component of the systems, respectively,

III. A SINGLE $\Xi_c\bar{D}^*$ ANALYSIS

With the above preparations, the OBE effective potential for the single $\Xi_c\bar{D}^*$ system is written as

$$\mathcal{V}_{\Xi_c\bar{D}^*} = 2I_B g_s \boldsymbol{\epsilon}_2 \cdot \boldsymbol{\epsilon}_4^\dagger Y(\Lambda, m_\sigma, r) - \frac{\mathcal{G}(I)}{4}\beta\beta_B g_v^2 \boldsymbol{\epsilon}_2 \cdot \boldsymbol{\epsilon}_4^\dagger Y(\Lambda, m_\rho, r) - \frac{1}{4}\beta\beta_B g_v^2 \boldsymbol{\epsilon}_2 \cdot \boldsymbol{\epsilon}_4^\dagger Y(\Lambda, m_\omega, r), \quad (20)$$

where $\mathcal{G}(I)$ is the isospin factor, its value is taken as 1 for the isospin-1 system, and -3 for the isospin-0 system. The function $Y(\Lambda, m, r)$ denotes

$$Y(\Lambda, m, r) = \frac{1}{4\pi r}(e^{-mr} - e^{-\Lambda r}) - \frac{\Lambda^2 - m^2}{8\pi\Lambda} e^{-\Lambda r}. \quad (21)$$

When performing the numerical calculations, the spin-spin operator $\mathcal{O}^{i,j}$ should be replaced by a serial of matrix elements $\langle {}^{2s'+1}L'_{J'}|\mathcal{O}^{i,j}|{}^{2s+1}L_J\rangle$, the $|{}^{2s+1}L_J\rangle$ and $|{}^{2s'+1}L'_{J'}\rangle$ stand for the spin-orbit wave functions for the initial and finial states, respectively. For example, the matrix elements $\langle f|\boldsymbol{\epsilon}_2 \cdot \boldsymbol{\epsilon}_4^\dagger|i\rangle$ for the $J^P = 1/2^-$ and $3/2^-$ $\Xi_c\bar{D}^*$ systems are diag(1,1,1) and diag(1,1,1,1) respectively when inputting the spin-orbit wave functions in Eq. (18). As we see, the OBE effective potentials are exactly the same for the $\Xi_c\bar{D}^*$ systems with $J^P = 1/2^-$ and $3/2^-$.

There exist σ, ρ, and ω exchange interactions for the single $\Xi_c\bar{D}^*$ system in Eq. (20). In Fig. 1, we present the corresponding S-wave effective potentials for the single $\Xi_c\bar{D}^*$ system with $I(J^P) = 0(1/2^-, 3/2^-)$. Here, the σ and ω exchanges provide an attractive and a repulsive interaction, respectively. The ρ exchange interaction is very different for the isoscalar and isovector $\Xi_c\bar{D}^*$ systems, i.e., for the isovector case, the ρ exchange provides a repulsive interaction, whereas a 3 times stronger attractive force exists in the isoscalar case.

After solving the Schrödinger equation, we find that bound solutions for the isoscalar $\Xi_c\bar{D}^*$ systems with $J^P = 1/2^-(3/2^-)$ appear in the range of $\Lambda > 2.00$ GeV.

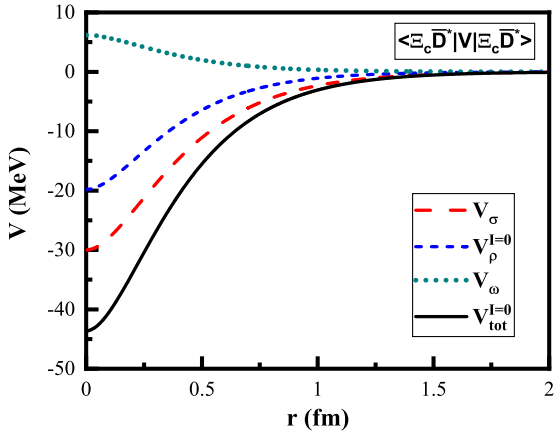

FIG. 1. The dependence of the S-wave OBE effective potentials for the isoscalar $\Xi_c\bar{D}^*$ system on r with $\Lambda = 1.00$ GeV.

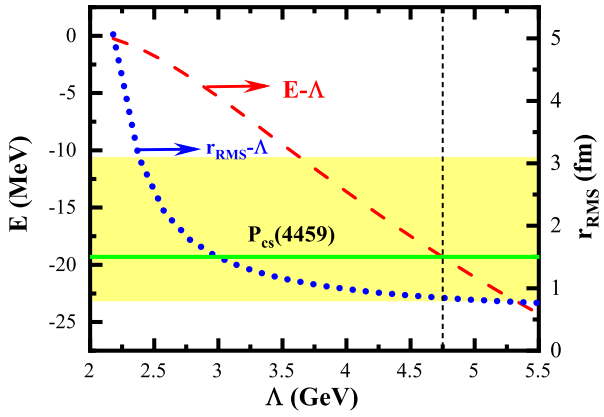

FIG. 2. The Λ dependence of the bound solutions (the binding energy E and the root-mean-square radius $r_{\rm rms}$) for the single $\Xi_c\bar{D}^*$ states. Here, the shadow area corresponds to the $P_{cs}(4459)$ mass with experimental uncertainties. The horizontal solid line and the vertical dotted line stand for the central mass of the $P_{cs}(4459)$ and the corresponding cutoff value.

With the increasing of the cutoff Λ, it binds more strongly. As shown in Fig. 2, when the cutoff Λ is taken in the range of $3.6 < \Lambda < 5.25$ GeV, we can reproduce the mass of the $P_{cs}(4459)$ with the experimental uncertainties. Obviously, the cutoff Λ is far away from the typical value 1.00 GeV in a loosely bound hadronic molecular state. Thus, our results indicate that the newly $P_{cs}(4459)$ cannot be a pure $\Xi_c\bar{D}^*$ molecule, although the total OBE effective potential is attractive.

Compared to the isoscalar $\Xi_c\bar{D}^*$ system, the OBE effective potential for the isovector system is much weaker attractive. We do not find the bound solutions in the range of $\Lambda < 5.00$ GeV.

In the $SU(3)$ flavor symmetry and heavy quark symmetry, the $\Xi_c\bar{D}^*$ is not related to the $\Sigma_c\bar{D}^*$ system but the $\Lambda_c\bar{D}^*$ system. Contrary to the $\Xi_c\bar{D}^*$ and $\Lambda_c\bar{D}^*$ systems, there exists the one-pion-exchange interaction in the $\Sigma_c\bar{D}^*$ system. Obviously, our results for the $\Xi_c\bar{D}^*$ state in a single channel analysis are also consistent with the predictions in Ref. [27], where Yang *et al.* found that there does not exist the S-wave $\Lambda_c\bar{D}^*$ molecular state, however, but the S-wave $\Sigma_c\bar{D}^*$ state with $I(J^P) = 1/2(3/2^-)$ which can be the possible hidden-charm molecular pentaquarks.

IV. A COUPLED $\Xi_c\bar{D}^*/\Xi_c^*\bar{D}/\Xi_c'\bar{D}^*/\Xi_c^*\bar{D}^*$ ANALYSIS

In this section, we further introduce the coupled channel effect to check whether the $P_{cs}(4459)$ can be explained as a strange hidden-charm molecular pentaquark. Here, we study the $\Xi_c\bar{D}^*/\Xi_c^*\bar{D}/\Xi_c'\bar{D}^*/\Xi_c^*\bar{D}^*$ interactions with $I(J^P) = 0, 1(1/2^-, 3/2^-)$. The total effective potentials are

$$V=\begin{pmatrix}\mathcal{V}^{11} & \mathcal{V}^{12} & \mathcal{V}^{13} & \mathcal{V}^{14}\\ \mathcal{V}^{21} & \mathcal{V}^{22} & \mathcal{V}^{23} & \mathcal{V}^{24}\\ \mathcal{V}^{31} & \mathcal{V}^{32} & \mathcal{V}^{33} & \mathcal{V}^{34}\\ \mathcal{V}^{41} & \mathcal{V}^{42} & \mathcal{V}^{43} & \mathcal{V}^{44}\end{pmatrix}$$
$$=\begin{pmatrix}\mathcal{V}^{\Xi_c\bar{D}^*\to\Xi_c\bar{D}^*} & \mathcal{V}^{\Xi_c^*\bar{D}\to\Xi_c\bar{D}^*} & \mathcal{V}^{\Xi_c'\bar{D}^*\to\Xi_c\bar{D}^*} & \mathcal{V}^{\Xi_c^*\bar{D}^*\to\Xi_c\bar{D}^*}\\ \mathcal{V}^{\Xi_c\bar{D}^*\to\Xi_c^*\bar{D}} & \mathcal{V}^{\Xi_c^*\bar{D}\to\Xi_c^*\bar{D}} & \mathcal{V}^{\Xi_c'\bar{D}^*\to\Xi_c^*\bar{D}} & \mathcal{V}^{\Xi_c^*\bar{D}^*\to\Xi_c^*\bar{D}}\\ \mathcal{V}^{\Xi_c\bar{D}^*\to\Omega_c^*\eta} & \mathcal{V}^{\Xi_c^*\bar{D}\to\Xi_c'\bar{D}^*} & \mathcal{V}^{\Xi_c'\bar{D}^*\to\Xi_c'\bar{D}^*} & \mathcal{V}^{\Xi_c^*\bar{D}^*\to\Xi_c'\bar{D}^*}\\ \mathcal{V}^{\Xi_c\bar{D}^*\to\Xi_c^*\bar{D}^*} & \mathcal{V}^{\Xi_c^*\bar{D}\to\Xi_c^*\bar{D}^*} & \mathcal{V}^{\Xi_c'\bar{D}^*\to\Xi_c^*\bar{D}^*} & \mathcal{V}^{\Xi_c^*\bar{D}^*\to\Xi_c^*\bar{D}^*}\end{pmatrix}. \tag{22}$$

The subpotentials are expressed as

$$\mathcal{V}^{11}=2\mathbb{A}\mathcal{Y}^{11}_{\Lambda,m_\sigma}-\frac{\mathbb{B}}{4}(\mathcal{G}(I)\mathcal{Y}^{11}_{\Lambda,m_\rho}+\mathcal{Y}^{11}_{\Lambda,m_\omega}), \tag{23}$$

$$\mathcal{V}^{12}=-\frac{\mathbb{C}}{6\sqrt{2}}(\mathcal{G}(I)\mathcal{Z}^{12}_{\Lambda_1,m_{\pi1}}+\mathcal{Z}^{12}_{\Lambda_1,m_{\eta1}})-\frac{\mathbb{D}}{6\sqrt{2}}(\mathcal{G}(I)\mathcal{Z}'^{12}_{\Lambda_1,m_{\rho1}}+\mathcal{Z}'^{12}_{\Lambda_1,m_{\omega1}}), \tag{24}$$

$$\mathcal{V}^{13}=\frac{\mathbb{C}}{6\sqrt{6}}(\mathcal{G}(I)\mathcal{Z}^{13}_{\Lambda_2,m_{\pi2}}+\mathcal{Z}^{13}_{\Lambda_2,m_{\eta2}})-\frac{\mathbb{D}}{3\sqrt{6}}(\mathcal{G}(I)\mathcal{Z}'^{13}_{\Lambda_2,m_{\rho2}}+\mathcal{Z}'^{13}_{\Lambda_2,m_{\omega2}}), \tag{25}$$

$$\mathcal{V}^{14}=-\frac{\mathbb{C}}{6\sqrt{2}}(\mathcal{G}(I)\mathcal{Z}^{14}_{\Lambda_3,m_{\pi3}}+\mathcal{Z}^{14}_{\Lambda_3,m_{\eta3}})+\frac{\mathbb{D}}{3\sqrt{2}}(\mathcal{G}(I)\mathcal{Z}'^{14}_{\Lambda_3,m_{\rho3}}+\mathcal{Z}'^{14}_{\Lambda_3,m_{\omega3}}), \tag{26}$$

$$\mathcal{V}^{22}=-\mathbb{A}'\mathcal{Y}^{22}_{\Lambda,m_\sigma}+\frac{\mathbb{B}'}{8}(\mathcal{G}(I)\mathcal{Y}^{22}_{\Lambda,m_\rho}+\mathcal{Y}^{22}_{\Lambda,m_\omega}), \tag{27}$$

$$\mathcal{V}^{23}=\frac{\mathbb{C}'}{8\sqrt{3}}\left(\mathcal{G}(I)\mathcal{Z}^{23}_{\Lambda_4,m_{\pi4}}-\frac{1}{3}\mathcal{Z}^{23}_{\Lambda_4,m_{\eta4}}\right)-\frac{\mathbb{D}'}{12\sqrt{3}}(\mathcal{G}(I)\mathcal{Z}'^{23}_{\Lambda_4,m_{\rho4}}+\mathcal{Z}'^{23}_{\Lambda_4,m_{\omega4}}), \tag{28}$$

$$\mathcal{V}^{24}=\frac{\mathbb{C}'}{8}\left(\mathcal{G}(I)\mathcal{Z}^{24}_{\Lambda_5,m_{\pi5}}-\frac{1}{3}\mathcal{Z}^{24}_{\Lambda_5,m_{\eta5}}\right)-\frac{\mathbb{D}'}{12}(\mathcal{G}(I)\mathcal{Z}'^{24}_{\Lambda_5,m_{\rho5}}+\mathcal{Z}'^{24}_{\Lambda_5,m_{\omega5}}), \tag{29}$$

$$\mathcal{V}^{33}=-\mathbb{A}'\mathcal{Y}^{33}_{\Lambda,m_\sigma}+\frac{\mathbb{C}'}{12}\left(\mathcal{G}(I)\mathcal{Z}^{33}_{\Lambda,m_\pi}-\frac{1}{3}\mathcal{Z}^{33}_{\Lambda,m_\eta}\right)-\frac{\mathbb{B}'}{8}(\mathcal{G}(I)\mathcal{Y}^{33}_{\Lambda,m_\rho}+\mathcal{Y}^{33}_{\Lambda,m_\omega})-\frac{\mathbb{D}'}{18}(\mathcal{G}(I)\mathcal{Z}'^{33}_{\Lambda,m_\rho}+\mathcal{Z}'^{33}_{\Lambda,m_\omega}), \tag{30}$$

$$\mathcal{V}^{34}=\frac{\mathbb{A}'}{\sqrt{3}}\mathcal{Y}^{34}_{\Lambda_6,m_{\sigma6}}+\frac{\mathbb{C}'}{8\sqrt{3}}\left(\mathcal{G}(I)\mathcal{Z}^{34}_{\Lambda_6,m_{\pi6}}-\frac{1}{3}\mathcal{Z}^{34}_{\Lambda_6,m_{\eta6}}\right)-\frac{\mathbb{B}'}{8\sqrt{3}}(\mathcal{G}(I)\mathcal{Y}^{34}_{\Lambda_6,m_{\rho6}}+\mathcal{Y}^{34}_{\Lambda_6,m_{\omega6}})-\frac{\mathbb{D}'}{12\sqrt{3}}(\mathcal{G}(I)\mathcal{Z}'^{34}_{\Lambda_6,m_{\rho6}}+\mathcal{Z}'^{34}_{\Lambda_6,m_{\omega6}}), \tag{31}$$

$$\mathcal{V}^{44}=-\mathbb{A}'\mathcal{Y}^{44}_{\Lambda,m_\sigma}-\frac{\mathbb{C}'}{8}\left(\mathcal{G}(I)\mathcal{Z}^{44}_{\Lambda,m_\pi}-\frac{1}{3}\mathcal{Z}^{44}_{\Lambda,m_\eta}\right)-\frac{\mathbb{B}'}{8}(\mathcal{G}(I)\mathcal{Y}^{44}_{\Lambda,m_\rho}+\mathcal{Y}^{44}_{\Lambda,m_\omega})-\frac{\mathbb{D}'}{12}(\mathcal{G}(I)\mathcal{Z}'^{44}_{\Lambda,m_\rho}+\mathcal{Z}'^{44}_{\Lambda,m_\omega}). \tag{32}$$

In the above expressions, we define several useful functions, i.e.,

$$\mathcal{Y}^{ij}_{\Lambda,m_a}=\mathcal{D}_{ij}Y(\Lambda,m_\sigma,r), \tag{33}$$

$$\mathcal{Z}^{ij}_{\Lambda,m_a}=\left(\mathcal{E}_{ij}\nabla^2+\mathcal{F}_{ij}r\frac{\partial}{\partial r}\frac{1}{r}\frac{\partial}{\partial r}\right)Y(\Lambda,m_a,r), \tag{34}$$

$$\mathcal{Z}'^{ij}_{\Lambda,m_a}=\left(2\mathcal{E}_{ij}\nabla^2-\mathcal{F}_{ij}r\frac{\partial}{\partial r}\frac{1}{r}\frac{\partial}{\partial r}\right)Y(\Lambda,m_a,r). \tag{35}$$

$\mathcal{D}_{ij}$, $\mathcal{E}_{ij}$, and $\mathcal{F}_{ij}$ stand for the spin-spin interaction and tensor force operators, the concrete expressions are summarized in the Appendix. The variables in these functions are defined as $\Lambda_i^2=\Lambda^2-q_i^2$, $m_i^2=m^2-q_i^2$, with $i=0,1,\ldots,6$. The coupling parameters and the values for q_i are summarized in Table II.

Here, we neglect the D-wave components for all discussed systems. After solving the coupled channel Schrödinger equation, we can only obtain bound states with their masses below the lowest threshold of the discussed channels. Here, we need to mention that one can further search for the possible resonances with higher masses by solving the scattering problems, which we leave to the next task. As we will see in the following results, we also take the cutoff value of cutoff from 1.00 to 5.00 GeV (see Table III for more details).

For the $I(J^P)=0(3/2^-)$ case, there exist bound state solutions with the cutoff around 1.00 GeV, and the $\Xi_c\bar{D}^*$ channel has a dominant contribution. It is obvious that the

TABLE II. Coupling parameters and the values for q_i adopted in our calculation. The unit for q_i is GeV.

$\mathbb{A}=l_Bg_s$	$\mathbb{B}=\beta\beta_Bg_v^2$	$\mathbb{C}=gg_4/f_\pi^2$	$\mathbb{D}=\lambda\lambda_Ig_v^2$
$\mathbb{A}'=l_sg_s$	$\mathbb{B}'=\beta\beta_sg_v^2$	$\mathbb{C}'=gg_1/f_\pi^2$	$\mathbb{D}'=\lambda\lambda_sg_v^2$
$q_1=0.16$	$q_2=0.06$	$q_3=0.10$	
$q_4=0.10$	$q_5=0.06$	$q_6=0.04$	

TABLE III. The obtained bound state solutions (the binding energy E, the root-mean-square $r_{\rm rms}$, the real binding energy $E_{\rm real} = E + M_{\rm lowest} - M_{\rm dominant}$, the mass of the bound state M, and the probabilities of different channels for the investigated system) of the coupled $\Xi_c\bar{D}^*/\Xi_c^*\bar{D}/\Xi_c'\bar{D}^*/\Xi_c^*\bar{D}^*$ systems with $I(J^P) = 0(1/2^-, 3/2^-)$. Here, the cutoff Λ, the root-mean-square $r_{\rm rms}$, the binding energy E, the real binding energy $E_{\rm real}$, and the mass of the bound state M are in the units of GeV and fm, MeV, MeV, and MeV, respectively. The dominant channels for a bound state are remarked by the boldface type.

$I(J^P)$	Λ	E	$r_{\rm rms}$	$E_{\rm real}$	M	$\Xi_c\bar{D}^*$	$\Xi_c^*\bar{D}$	$\Xi_c'\bar{D}^*$	$\Xi_c^*\bar{D}^*$
$0(1/2^-)$	1.17	−1.63	1.39	−109.04	4476.32	30.66	⋯	**64.13**	5.21
	1.18	−7.52	0.62	−114.93	4470.43	15.82	⋯	**77.10**	7.08
	1.19	−14.29	0.50	−121.70	4463.66	11.12	⋯	**80.82**	8.06
	1.20	−21.62	0.45	−129.03	4456.33	8.60	⋯	**82.62**	8.78
$0(3/2^-)$	0.99	−1.46	2.18	−1.46	4476.49	**69.44**	19.46	2.81	8.28
	1.01	−5.73	1.09	−5.73	4472.22	**53.70**	28.41	5.52	13.37
	1.03	−11.77	0.79	−11.77	4466.18	**44.88**	**32.50**	5.69	16.93
	1.05	−19.28	0.65	−19.28	4458.67	**38.95**	**34.58**	6.61	18.86

value of the cutoff for the coupled channel case is smaller than that for the single channel case. Thus, we can conclude that the coupled channel effect is helpful to form this bound state. We also notice that its root-mean-square (rms) radius is around 1 fm when the binding energy varies from 0 to −10 MeV, the size is reasonable for such a coupled $\Xi_c\bar{D}^*/\Xi_c^*\bar{D}/\Xi_c'\bar{D}^*/\Xi_c^*\bar{D}^*$ molecular system. As it binds deeper and deeper, the $\Xi_c^*\bar{D}$ component becomes more and more important. In particular, when the cutoff Λ is taken as 1.05 GeV, one can reproduce the central mass of the newly $P_{cs}(4459)$, the probabilities for both $\Xi_c\bar{D}^*$ and $\Xi_c^*\bar{D}$ channels are over 30 percent.

When the cutoff is taking from 1.17 to 1.20 GeV, we can obtain a loosely bound state for the $I(J^P) = 0(1/2^-)$ case. Here, the $\Xi_c'\bar{D}^*$ channel is its dominant channel. The "real" binding energy is over 100 MeV in the range of $1.17 < \Lambda < 1.20$ GeV. Where the real binding energy $E_{\rm real}$ is $E_{\rm real} = E + M_{\rm lowest} - M_{\rm dominant}$, $M_{\rm lowest}$ and $M_{\rm dominant}$ are the mass thresholds of the channel with lowest mass and the dominant channel, respectively. Although the cutoff is reasonable, the corresponding rms radius is only around or less than 0.5 fm when reproducing the mass of $P_{cs}(4459)$. It is obvious that the molecular state picture with the $I(J^P) = 0(1/2^-)$ assignment to $P_{cs}(4459)$ is not favored.

To summarize, the coupled $\Xi_c\bar{D}^*/\Xi_c^*\bar{D}/\Xi_c'\bar{D}^*/\Xi_c^*\bar{D}^*$ state with $I(J^P) = 0(3/2^-)$ can be a possible strange hidden-charm molecular candidate, the $\Xi_c\bar{D}^*$ and $\Xi_c^*\bar{D}$ channels are dominant, followed by the $\Xi_c^*\bar{D}^*$ channel. It may relate to the new $P_{cs}(4459)$ recently reported by the LHCb collaboration. Here, we also obtain bound state solutions for the coupled $\Xi_c\bar{D}^*/\Xi_c^*\bar{D}/\Xi_c'\bar{D}^*/\Xi_c^*\bar{D}^*$ system with $I(J^P) = 0(1/2^-)$, its real binding energy reaches around 100 MeV as the dominant channel is the $\Xi_c'\bar{D}^*$ channel, thus, the relevant OBE interaction from the $\Xi_c'\bar{D}^*$ system is strongly attractive. Although it is not a reasonable loose hadronic molecular candidate, in our future study, we can search for possible loosely bound strange hidden-charm molecules near the threshold of the $\Xi_c'\bar{D}^*$ system.

As a by-product, we further discuss the existence of the isovector strange hidden-charm molecular pentaquarks from the S-wave $\Xi_c\bar{D}^*/\Xi_c^*\bar{D}/\Xi_c'\bar{D}^*/\Xi_c^*\bar{D}^*$ interactions. According to the numerical results in Table IV, we find the $I(J^P) = 1(1/2^-)\Xi_c\bar{D}^*/\Xi_c^*\bar{D}/\Xi_c'\bar{D}^*/\Xi_c^*\bar{D}^*$ state is a tight bound state; the $\Xi_c^*\bar{D}^*$ channel is the dominant

TABLE IV. The obtained bound state solutions (the binding energy E, the root-mean-square $r_{\rm rms}$, the real binding energy $E_{\rm real} = E + M_{\rm lowest} - M_{\rm dominant}$, the mass of the bound state M, and the probabilities of different channels for the investigated system) of the coupled $\Xi_c\bar{D}^*/\Xi_c^*\bar{D}/\Xi_c'\bar{D}^*/\Xi_c^*\bar{D}^*$ systems with $I(J^P) = 1(1/2^-, 3/2^-)$. Here, the cutoff Λ, the root-mean-square $r_{\rm rms}$, the binding energy E, the real binding energy $E_{\rm real}$, and the mass of the bound state M are in the units of GeV and fm, MeV, MeV, and MeV, respectively. The dominant channels for a bound state are remarked by the boldface type.

$I(J^P)$	Λ	E	$r_{\rm rms}$	$E_{\rm real}$	M	$\Xi_c\bar{D}^*$	$\Xi_c^*\bar{D}$	$\Xi_c'\bar{D}^*$	$\Xi_c^*\bar{D}^*$
$1(1/2^-)$	2.07	−2.05	0.36	−178.56	4475.90	5.80	⋯	5.33	**88.87**
	2.08	−16.84	0.24	−193.35	4461.11	5.03	⋯	5.30	**89.67**
	2.09	−32.20	0.23	−208.71	4445.75	4.95	⋯	5.23	**89.81**
	2.10	−48.12	0.22	−224.63	4429.83	4.95	⋯	5.17	**89.88**
$1(3/2^-)$	1.43	−1.62	0.94	−36.78	4476.33	12.96	**80.10**	0.61	6.34
	1.44	−5.68	0.67	−40.84	4472.27	9.92	**82.29**	0.64	7.14
	1.45	−10.12	0.60	−45.28	4467.83	9.12	**82.41**	0.66	7.81
	1.46	−14.91	0.57	−50.07	4463.04	8.78	**82.08**	0.67	8.47

channel. However, we need to specify that the cutoff Λ is a little bit larger than 1 GeV. For the $I(J^P) = 1(3/2^-)$ case, when the cutoff reaches up to 1.43 GeV, we can obtain a bound state, where the $\Xi_c^*\bar{D}$ channel is dominant. If strictly taking Λ around 1 GeV and the rms radius around 1 fm, we may predict there is a possible strange hidden-charm $\Xi_c^*\bar{D}$ molecular candidate.

In our former work [6], we study the $\Sigma_c\bar{D}/\Sigma_c^*\bar{D}/\Sigma_c\bar{D}^*/\Sigma_c^*\bar{D}^*$ interactions by using the same approach. When we take the same cutoff range around 1 GeV, we find the $P_c(4312)$, $P_c(4440)$, and $P_c(4457)$ can be explained as hidden-charm molecular pentaquarks, the corresponding dominant channels are the $\Sigma_c\bar{D}$ state with $1/2(1/2^-)$, the $\Sigma_c\bar{D}^*$ states with $1/2(1/2^-)$ and $1/2(3/2^-)$, respectively. Based on the above analysis, the new $P_{cs}(4457)$ can be naturally assigned as a strange hidden-charm molecular pentaquark.

V. SUMMARY

Inspired by the evidence of the first strange hidden-charm pentaquark $P_{cs}(4459)$, we systematically discuss whether the $P_{cs}(4459)$ can be assigned as the $\Xi_c\bar{D}^*$ molecular state. In this work, we adopt the OBE effective potentials and present our results in two cases.

In case one, we study the single $\Xi_c\bar{D}^*$ system and consider the $S-D$ wave mixing effect. The long range interaction from the one-π-exchange is suppressed by the spin parity forbidden. There remain the intermediate range force from the one-σ-exchange and the short range force from the one-ρ/ω-exchange. The OBE effective potentials for the $I(J^P) = 0(1/2^-, 3/2^-)$ are exactly the same. Our results indicate the OBE effective potentials are not strong enough to form a single $\Xi_c\bar{D}^*$ system.

In case two, we further study the coupled $\Xi_c\bar{D}^*/\Xi_c^*\bar{D}/\Xi_c'\bar{D}^*/\Xi_c^*\bar{D}^*$ systems with $I(J^P) = 0(1/2^-, 3/2^-)$ after introducing the coupled channel effect. Finally, we obtain a good strange hidden-charm molecular pentaquark with $I(J^P) = 0(3/2^-)$, it is mainly composed by the $\Xi_c\bar{D}^*$ and $\Xi_c^*\bar{D}$ channels. The coupled channel effect plays an important role here. When the cutoff is taken as $\Lambda = 1.05$ GeV, we can reproduce the central mass of the $P_{cs}(4459)$, and the probabilities for the $\Xi_c\bar{D}^*$, $\Xi_c^*\bar{D}$, $\Xi_c'\bar{D}^*$, and $\Xi_c^*\bar{D}^*$ channels are 38.95%, 34.58%, 6.61%, and 18.86%, respectively.

In addition, we also find the OBE effective potentials for the $\Xi_c'\bar{D}^*$ system with $0(1/2^-)$ and the $\Xi_c^*\bar{D}$ system with $1(3/2^-)$ are strongly attractive in the reasonable cutoff input, where one may search for more possible strange hidden-charm molecules or resonances.

ACKNOWLEDGMENTS

Rui Chen is very grateful to Xiang Liu and Shi-Lin Zhu for helpful discussions and constructive suggestions. This project is supported by the National Postdoctoral Program for Innovative Talent.

APPENDIX: OPERATORS

The concrete operators in the OBE effective potentials are

$$\mathcal{D}_{11} = \chi_3^\dagger\chi_1\boldsymbol{\epsilon}_2\cdot\boldsymbol{\epsilon}_4^\dagger,$$
$$\mathcal{E}_{12} = \sum_{m,n} C^{3/2,m+n}_{1/2,m;1,n}\chi_{3,m}^\dagger\boldsymbol{\epsilon}_{3,n}^\dagger\cdot\boldsymbol{\epsilon}_2\chi_1,$$
$$\mathcal{F}_{12} = \sum_{m,n} C^{3/2,m+n}_{1/2,m;1,n}\chi_{3,m}^\dagger S(\hat{r},\boldsymbol{\epsilon}_{3,n}^\dagger,\boldsymbol{\epsilon}_2)\chi_1,$$
$$\mathcal{E}_{13} = \chi_3^\dagger\boldsymbol{\sigma}\cdot(i\boldsymbol{\epsilon}_2\times\boldsymbol{\epsilon}_4^\dagger)\chi_1,$$
$$\mathcal{F}_{13} = \chi_3^\dagger S(\hat{r},\boldsymbol{\sigma},i\boldsymbol{\epsilon}_2\times\boldsymbol{\epsilon}_4^\dagger)\chi_1,$$
$$\mathcal{E}_{14} = \sum_{m,n} C^{3/2,m+n}_{1/2,m;1,n}\chi_{3,m}^\dagger(i\boldsymbol{\epsilon}_2\times\boldsymbol{\epsilon}_4^\dagger)\cdot\boldsymbol{\epsilon}_{3,n}^\dagger\chi_1,$$
$$\mathcal{F}_{14} = \sum_{m,n} C^{3/2,m+n}_{1/2,m;1,n}\chi_{3,m}^\dagger S(\hat{r},\boldsymbol{\epsilon}_{3,n}^\dagger,i\boldsymbol{\epsilon}_2\times\boldsymbol{\epsilon}_4^\dagger)\chi_1,$$
$$\mathcal{D}_{22} = \sum_{a,b}^{m,n} C^{3/2,a+b}_{1/2,a;1,b}C^{3/2,m+n}_{1/2,m;1,n}\chi_3^{a\dagger}\chi_1^m\boldsymbol{\epsilon}_1^n\cdot\boldsymbol{\epsilon}_3^{b\dagger},$$
$$\mathcal{E}_{32} = \sum_{m,n} C^{3/2,m+n}_{1/2,m;1,n}\chi_3^\dagger\boldsymbol{\epsilon}_4^\dagger\cdot(i\boldsymbol{\sigma}\times\boldsymbol{\epsilon}_1^n)\chi_{1,m},$$
$$\mathcal{F}_{32} = \sum_{m,n} C^{3/2,m+n}_{1/2,m;1,n}\chi_3^\dagger S(\hat{r},\boldsymbol{\epsilon}_4^\dagger,i\boldsymbol{\sigma}\times\boldsymbol{\epsilon}_1^n)\chi_{1,m},$$
$$\mathcal{E}_{42} = \sum_{a,b}^{m,n} C^{3/2,a+b}_{1/2,a;1,b}C^{3/2,m+n}_{1/2,m;1,n}\chi_3^{a\dagger}\chi_1^m\boldsymbol{\epsilon}_4^\dagger\cdot(i\boldsymbol{\epsilon}_1^n\times\boldsymbol{\epsilon}_3^{b\dagger}),$$
$$\mathcal{F}_{42} = \sum_{a,b}^{m,n} C^{3/2,a+b}_{1/2,a;1,b}C^{3/2,m+n}_{1/2,m;1,n}\chi_3^{a\dagger}\chi_1^m S(\hat{r},\boldsymbol{\epsilon}_4^\dagger,i\boldsymbol{\epsilon}_1^n\times\boldsymbol{\epsilon}_3^{b\dagger}),$$
$$\mathcal{D}_{33} = \chi_3^\dagger\chi_1\boldsymbol{\epsilon}_2\cdot\boldsymbol{\epsilon}_4^\dagger,$$
$$\mathcal{E}_{33} = \chi_3^\dagger\boldsymbol{\sigma}\cdot(i\boldsymbol{\epsilon}_2\times\boldsymbol{\epsilon}_4^\dagger)\chi_1,$$
$$\mathcal{F}_{33} = \chi_3^\dagger S(\hat{r},\boldsymbol{\sigma},i\boldsymbol{\epsilon}_2\times\boldsymbol{\epsilon}_4^\dagger)\chi_1,$$
$$\mathcal{D}_{43} = \sum_{m,n} C^{\frac{3}{2},m+n}_{\frac{1}{2},m;1,n}\chi_3^{m\dagger}(\boldsymbol{\sigma}\cdot\boldsymbol{\epsilon}_3^{n\dagger})(\boldsymbol{\epsilon}_2\cdot\boldsymbol{\epsilon}_4^\dagger)\chi_1,$$
$$\mathcal{E}_{43} = \sum_{m,n} C^{\frac{3}{2},m+n}_{\frac{1}{2},m;1,n}\chi_3^{m\dagger}(\boldsymbol{\sigma}\times\boldsymbol{\epsilon}_3^{n\dagger})\cdot(\boldsymbol{\epsilon}_2\times\boldsymbol{\epsilon}_4^\dagger)\chi_1,$$
$$\mathcal{F}_{43} = \sum_{m,n} C^{\frac{3}{2},m+n}_{\frac{1}{2},m;1,n}\chi_3^{m\dagger} S(\hat{r},\boldsymbol{\sigma}\times\boldsymbol{\epsilon}_3^{n\dagger},\boldsymbol{\epsilon}_2\times\boldsymbol{\epsilon}_4^\dagger)\chi_1,$$
$$\mathcal{D}_{44} = \sum_{a,b}^{m,n} C^{\frac{3}{2},a+b}_{\frac{1}{2},a;1,b}C^{\frac{3}{2},m+n}_{\frac{1}{2},m;1,n}\chi_3^{a\dagger}(\boldsymbol{\epsilon}_1^n\cdot\boldsymbol{\epsilon}_3^{b\dagger})(\boldsymbol{\epsilon}_2\cdot\boldsymbol{\epsilon}_4^\dagger)\chi_1^m,$$
$$\mathcal{E}_{44} = \sum_{a,b}^{m,n} C^{\frac{3}{2},a+b}_{\frac{1}{2},a;1,b}C^{\frac{3}{2},m+n}_{\frac{1}{2},m;1,n}\chi_3^{a\dagger}(\boldsymbol{\epsilon}_1^n\times\boldsymbol{\epsilon}_3^{b\dagger})\cdot(\boldsymbol{\epsilon}_2\times\boldsymbol{\epsilon}_4^\dagger)\chi_1^m,$$
$$\mathcal{F}_{44} = \sum_{a,b}^{m,n} C^{\frac{3}{2},a+b}_{\frac{1}{2},a;1,b}C^{\frac{3}{2},m+n}_{\frac{1}{2},m;1,n}\chi_3^{a\dagger} S(\hat{r},\boldsymbol{\epsilon}_1^n\times\boldsymbol{\epsilon}_3^{b\dagger},\boldsymbol{\epsilon}_2\times\boldsymbol{\epsilon}_4^\dagger)\chi_1^m.$$

[1] R. Aaij *et al.* (LHCb Collaboration), Phys. Rev. Lett. **122**, 222001 (2019).
[2] R. Aaij *et al.* (LHCb Collaboration), Phys. Rev. Lett. **115**, 072001 (2015).
[3] R. Chen, X. Liu, X. Q. Li, and S. L. Zhu, Phys. Rev. Lett. **115**, 132002 (2015).
[4] H. X. Chen, W. Chen, X. Liu, T. G. Steele, and S. L. Zhu, Phys. Rev. Lett. **115**, 172001 (2015).
[5] L. Roca, J. Nieves, and E. Oset, Phys. Rev. D **92**, 094003 (2015).
[6] R. Chen, Z. F. Sun, X. Liu, and S. L. Zhu, Phys. Rev. D **100**, 011502 (2019).
[7] M. Z. Liu, Y. W. Pan, F. Z. Peng, M. Sanchez Sanchez, L. S. Geng, A. Hosaka, and M. Pavon Valderrama, Phys. Rev. Lett. **122**, 242001 (2019).
[8] J. He, Eur. Phys. J. C **79**, 393 (2019).
[9] L. Meng, B. Wang, G. J. Wang, and S. L. Zhu, Phys. Rev. D **100**, 014031 (2019).
[10] T. J. Burns and E. S. Swanson, Phys. Rev. D **100**, 114033 (2019).
[11] J. Ferretti, E. Santopinto, M. Naeem Anwar, and M. A. Bedolla, Phys. Lett. B **789**, 562 (2019).
[12] L. Maiani, A. D. Polosa, and V. Riquer, Phys. Lett. B **749**, 289 (2015).
[13] R. F. Lebed, Phys. Lett. B **749**, 454 (2015).
[14] X. Z. Weng, X. L. Chen, W. Z. Deng, and S. L. Zhu, Phys. Rev. D **100**, 016014 (2019).
[15] A. Ali and A. Y. Parkhomenko, Phys. Lett. B **793**, 365 (2019).
[16] J. F. Giron, R. F. Lebed, and C. T. Peterson, J. High Energy Phys. 05 (2019) 061.
[17] J. B. Cheng and Y. R. Liu, Phys. Rev. D **100**, 054002 (2019).
[18] H. Mutuk, Chin. Phys. C **43**, 093103 (2019).
[19] F. K. Guo, U. G. Meißner, W. Wang, and Z. Yang, Phys. Rev. D **92**, 071502 (2015).
[20] X. H. Liu, Q. Wang, and Q. Zhao, Phys. Lett. B **757**, 231 (2016).
[21] H. X. Chen, W. Chen, X. Liu, and S. L. Zhu, Phys. Rep. **639**, 1 (2016).
[22] Y. R. Liu, H. X. Chen, W. Chen, X. Liu, and S. L. Zhu, Prog. Part. Nucl. Phys. **107**, 237 (2019).
[23] N. Brambilla, S. Eidelman, C. Hanhart, A. Nefediev, C. P. Shen, C. E. Thomas, A. Vairo, and C. Z. Yuan, Phys. Rep. **873**, 1 (2020).
[24] F. K. Guo, C. Hanhart, U. G. Meißner, Q. Wang, Q. Zhao, and B. S. Zou, Rev. Mod. Phys. **90**, 015004 (2018).
[25] A. Esposito, A. Pilloni, and A. D. Polosa, Phys. Rep. **668**, 1 (2017).
[26] A. Hosaka, T. Iijima, K. Miyabayashi, Y. Sakai, and S. Yasui, Prog. Theor. Exp. Phys. **2016**, 062C01 (2016).
[27] Z. C. Yang, Z. F. Sun, J. He, X. Liu, and S. L. Zhu, Chin. Phys. C **36**, 6 (2012).
[28] J. J. Wu, R. Molina, E. Oset, and B. S. Zou, Phys. Rev. Lett. **105**, 232001 (2010).
[29] W. L. Wang, F. Huang, Z. Y. Zhang, and B. S. Zou, Phys. Rev. C **84**, 015203 (2011).
[30] M. Karliner and J. L. Rosner, Phys. Rev. Lett. **115**, 122001 (2015).
[31] X. Q. Li and X. Liu, Eur. Phys. J. C **74**, 3198 (2014).
[32] M. Z. Wang, On behalf of the LHCb collaboration at Implications workshop 2020, see https://indico.cern.ch/event/857473/timetable/32-exotic-hadrons-experimental.
[33] H. X. Chen, W. Chen, X. Liu, and X. H. Liu, arXiv:2011.01079.
[34] F. Z. Peng, M. J. Yan, M. Sánchez Sánchez, and M. P. Valderrama, arXiv:2011.01915.
[35] Z. G. Wang, arXiv:2011.05102.
[36] J. J. Wu, R. Molina, E. Oset, and B. S. Zou, Phys. Rev. C **84**, 015202 (2011).
[37] B. Wang, L. Meng, and S. L. Zhu, Phys. Rev. D **101**, 034018 (2020).
[38] V. V. Anisovich, M. A. Matveev, J. Nyiri, A. V. Sarantsev, and A. N. Semenova, Int. J. Mod. Phys. A **30**, 1550190 (2015).
[39] Z. G. Wang, Eur. Phys. J. C **76**, 142 (2016).
[40] A. Feijoo, V. K. Magas, A. Ramos, and E. Oset, Eur. Phys. J. C **76**, 446 (2016).
[41] J. X. Lu, E. Wang, J. J. Xie, L. S. Geng, and E. Oset, Phys. Rev. D **93**, 094009 (2016).
[42] R. Chen, J. He, and X. Liu, Chin. Phys. C **41**, 103105 (2017).
[43] C. W. Xiao, J. Nieves, and E. Oset, Phys. Lett. B **799**, 135051 (2019).
[44] Q. Zhang, B. R. He, and J. L. Ping, arXiv:2006.01042.
[45] C. W. Shen, H. J. Jing, F. K. Guo, and J. J. Wu, Symmetry **12**, 1611 (2020).
[46] J. Ferretti and E. Santopinto, J. High Energy Phys. 04 (2020) 119.
[47] H. X. Chen, L. S. Geng, W. H. Liang, E. Oset, E. Wang, and J. J. Xie, Phys. Rev. C **93**, 065203 (2016).
[48] T. M. Yan, H. Y. Cheng, C. Y. Cheung, G. L. Lin, Y. C. Lin, and H. L. Yu, Phys. Rev. D **46**, 1148 (1992); **55**, 5851(E) (1997).
[49] M. B. Wise, Phys. Rev. D **45**, R2188 (1992).
[50] G. Burdman and J. F. Donoghue, Phys. Lett. B **280**, 287 (1992).
[51] R. Casalbuoni, A. Deandrea, N. Di Bartolomeo, R. Gatto, F. Feruglio, and G. Nardulli, Phys. Rep. **281**, 145 (1997).
[52] A. F. Falk and M. E. Luke, Phys. Lett. B **292**, 119 (1992).
[53] Y. R. Liu and M. Oka, Phys. Rev. D **85**, 014015 (2012).
[54] W. A. Bardeen, E. J. Eichten, and C. T. Hill, Phys. Rev. D **68**, 054024 (2003).
[55] C. Isola, M. Ladisa, G. Nardulli, and P. Santorelli, Phys. Rev. D **68**, 114001 (2003).
[56] P. A. Zyla *et al.* (Particle Data Group), Prog. Theor. Exp. Phys. **2020**, 083C01 (2020).
[57] R. Chen, A. Hosaka, and X. Liu, Phys. Rev. D **96**, 116012 (2017).
[58] N. A. Tornqvist, Z. Phys. C **61**, 525 (1994).
[59] N. A. Tornqvist, Nuovo Cimento A **107**, 2471 (1994).